Journal of the European Ceramic Society 22 (2002) 1653–1660

www.elsevier.com/locate/jeurceramsoc

Varistor behaviour of Mn-doped ZnO ceramics

Jiaping Han, A.M.R. Senos, P.Q. Mantas*

Department of Ceramic and Glass Engineering/UIMC, University of Aveiro, 3810-193 Aveiro, Portugal

Received 28 March 2001; received in revised form 20 September 2001; accepted 26 September 2001

Abstract

Polycrystalline ZnO doped with MnO, from 0.1 to 0.6 mol%, was prepared by conventional ceramic processing. The effect of Mn doping on the electrical properties of ZnO was investigated. Samples quenched from the sintering temperature show ohmic behaviour, while pronounced varistor behaviour is found in Mn-doped ZnO obtained by slow cooling from the sintering temperature or by annealing at a lower temperature. The origin of the varistor effect in the samples of polycrystalline ZnO with MnO as the only additive is discussed. The defect equilibrium analysis suggests that the varistor behaviour in these samples is due to the oxidation of the double ionised zinc interstitial defects present at grain boundaries by ambient oxygen during cooling or annealing, and the presence of Mn in the ZnO grains induces this process.

Keywords: Electrical conductivity; Impurities; Sintering; Varistors; ZnO

1. Introduction

A typical ZnO based varistor is a very complex chemical system that contains several dopants, such as Bi_2O_3, CoO, MnO, Sb_2O_3, and Cr_2O_3.[1–4] It has been proposed that the dopants responsible for the formation of the varistor behaviour are cations of large ionic radii, with low solubility in ZnO at low temperature, like Bi, Pr, Ba, Sr, or Ca.[1–4] These dopants are often called "varistor formers". The other dopants are added for improving the nonohmic properties, such as CoO and MnO, or the densification of ceramics and their reliability, such as Sb_2O_3 and Cr_2O_3. Several studies have been done to investigate the role of the various additives on the microstructure development and electrical properties of ZnO varistors.[1–4] However, the contribution of each additive has often been considered within the multicomponent system. Because of the very complex composition and microstructure, it is difficult to investigate the specific role of each dopant in the multicomponent system. The purpose of the present work is to investigate the effect of the Mn doping on the electrical properties of ZnO ceramics in binary system.

In a previous work,[5] we have sintered undoped and Mn-doped ZnO samples (0.1, 0.3 and 0.6 mol% MnO) at three temperatures (1100, 1200 and 1300 °C), for 2 h in air, and then quenched them to room temperature. With this procedure, we tried to avoid any defect diffusion to the grain boundaries or the reaction of grain boundary (GB) defects with ambient oxygen during cooling, in order to evaluate the effect of Mn on the defect chemistry of ZnO. We arrived at the conclusion that Mn is a deep donor in ZnO with an ionisation energy of around ~2.0 eV at room temperature, and that it significantly depresses the concentration of the intrinsic donors, the interstitial zinc, during sintering. Consequently, Mn makes ZnO a more resistive material at room temperature. Up to 0.6 mol% of MnO, we did not observe any non-linear behaviour on the I–V curves of these quenched samples at room temperature. We could then state that Mn plays no direct role on the conductivity of ZnO at room temperature, since it is a deep donor, but it controls the carrier density through the interference on the concentration of the intrinsic donor defect. A similar conclusion was drawn by Einzinger,[6] who stated that deep donors shift the concentrations of the intrinsic defects at the GBs, decreasing the donor concentration and increasing the acceptor one, in such an amount that electrical barriers can be built up in those regions. In this paper, we prepared samples in the same way as reported before,[5] but

* Corresponding author. Tel.: +351-234-370-268; fax: +351-234-425-300.

E-mail address: pmantas@cv.ua.pt (P.Q. Mantas).

0955-2219/02/$ - see front matter
PII: S0955-2219(01)00484-8

allowing them to slowly cool to room temperature, instead of being quenched.

2. Experimental procedure

The Reagent grade ZnO powders (Aldrich, Milwaukee, WI) with 99.9% purity and mean particle size of 0.26 μm was used. To dope with Mn, alcohol solutions of hydrated manganese nitrate ($Mn(NO_3)_2.4H_2O$) were prepared and mixed with ZnO powder in a planetary milling for 4 h using a plastic container without balls. The amount of manganese ranged from 0.1 to 0.6 mol%. The slurry was dried at 80 °C, and the obtained powder was calcined at 450 °C for 1 h. Disk-shaped specimens of 10 mm diameter and 1–2 mm height were obtained by uniaxial pressing at 100 MPa, followed by isostatic pressing at 200 MPa.

Sintering was performed in air. In the case of the quenched samples, a tube furnace was raise up to 1200 °C, and then the specimens were quickly inserted in the centre of the furnace. After being sintered for 2 h, the samples were quenched in air. These samples will be denoted as *quenched samples*. Slowly cooled samples were heated up to 1200 °C at constant heating rate of 5 °C/min. After 2 h at 1200 °C, the samples were cooled to 600 °C at the rate of 1 °C/min, and then furnace cooled to room temperature. These samples will be called *slowly cooled samples*. Quenched samples were later annealed at 800 °C for 2 h in air, and then furnace cooled to room temperature. These samples will be called *annealed samples*.

The densities of the specimens were determined by the Hg-immersion method. X-ray diffractometry (XRD, Model Geigerflex D, Rigaku Co., Japan) was used for phase analyses of the sintered specimens. The microstructures of the sintered specimens were characterised by a scanning electron microscope (SEM, Model S-4100, Hitachi, Japan) after polishing and thermal etching. The grain sizes were measured from SEM photomicrographs using an image analysis system (Model Quantimet 500+, Leica Cambridge Ltd, UK). The average grain sizes were obtained by the Schwartz-Saltykov method.[7] Transmission electron microscopy (TEM, Model H-9000, Hitachi, Japan) was performed at 300 kV to further analyse the microstructures of the sintered specimens which were mechanical-polished and ion-thinned.

Specimens for electrical measurement were polished with 1200-grit SiC on both sides, ultrasonically cleaned, and then electroded by sputtering gold or covering with In–Ga alloy. Electrical current-voltage behaviour were measured with an electrometer (Model 617, Keithley, USA) and a current source (Model 220, Keithley, USA), up to 100 V. For higher voltages, a pulsed voltage source (AMBO, with 60 μs pulse duration, 13 Hz, up to 1 kV) and an oscilloscope (Model PM3082, Philips, Netherlands) were used.

3. Results

Fig. 1 shows the SEM microstructures of the slowly cooled samples of undoped and Mn-doped ZnO. In the case of Mn-doped samples, no second phase is observed from these micrographs. The X-ray diffraction patterns of all the samples show that only single ZnO phase is present. No second phase could also be observed by TEM. The same feature is also true for the quenched and annealed samples from SEM, TEM, and XRD analyses.

In Fig. 1, all the slowly cooled samples show uniform equiaxed grains and no abnormal grain growth. Similar microstructures are observed in the quenched and annealed samples. The average grain sizes of all the samples are between 5 and 10 μm, and the sintered relative densities of the samples range between 95 and 97%. With the increase in the Mn doping level, the average grain size increases, but the densities change slightly. The grain growth and the densification of Mn-doped ZnO were analysed in previous works.[8,9] It could be found that, Mn doping reduces the densification rate of ZnO in the early stage of sintering,[8] while in the intermediate and final stages of sintering, it promotes the grain growth of ZnO.[9]

As presented in a previous work,[5] trace element analysis by inductively coupled plasma emission spectroscopy in the sintered samples indicates that the concentration of each background impurity of Bi, Ba, Sr, Ca, Pb, Co, Sb, Cu, Al, and Na, is very low (<16 ppm) and much lower than the Mn doping level.

Fig. 2 shows the dc J–E (current density-electric field) characteristics of undoped and Mn-doped ZnO samples sintered at 1200 °C for 2 h: (a) slowly cooled, (b) quenched, and (c) annealed samples. Non-linear J–E characteristics are observed in the slowly cooled and annealed samples with Mn doping, whereas the quenched samples and all undoped ZnO samples show ohmic behaviour. These J–E characteristics are independent of the electrode type (either Au or In–Ga alloy electrodes), and the resistivities of the low voltage region are proportional to the sample thickness. In the breakdown region of the J–E curves, it is common to define the curves by an empirical relation of the type[1–3]

$$I = KV^{\alpha} \tag{1}$$

where K is a proportional factor and α the non-linear coefficient. α was determined in the window of current densities of 10^{-3}–10^{-1} A/cm^2. The leakage current density was defined as the current density for an electric field of 1 V/cm. The average grain size, the nonlinear coefficient, α, and the leakage current density of these samples are summarised in Table 1. The cooled sample doped with 0.3 mol% MnO has the largest nonlinearity coefficient, $\alpha = 7.5$, which is higher than that obtained by ZnO doped with only Bi_2O_3.[10]

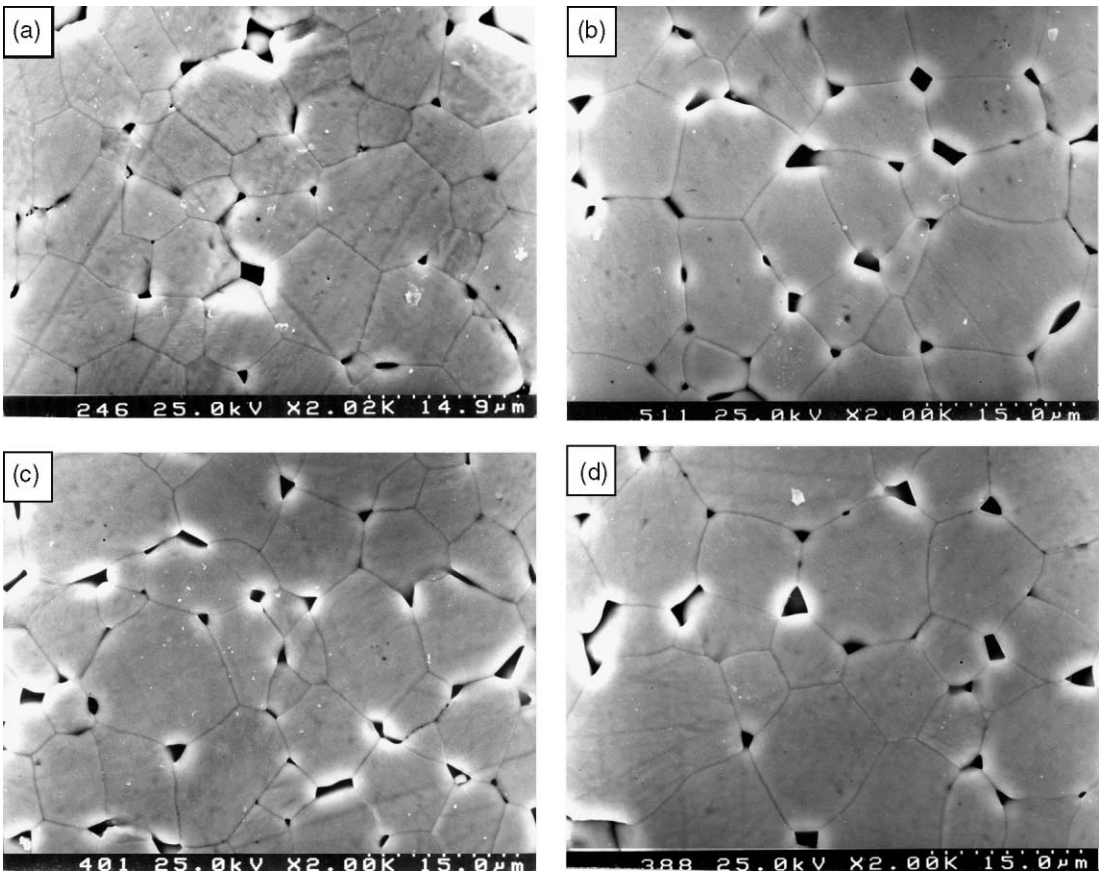

Fig. 1. Microstructure of undoped and Mn-doped ZnO sintered at 1200 °C for 2 h and then slowly cooled, for (a) undoped ZnO, (b) 0.1 mol% MnO, (c) 0.3 mol% MnO, and (d) 0.6 mol% MnO.

Table 1
Average grain size, nonlinear coefficient, and leakage current density of Mn-doped ZnO samples slowly cooled from the sintering temperature (1200 °C) or annealed at 800 °C

Composition	Average grain size (μm)	Nonlinear coefficient	Leakage current density (A/cm^2) at IV/cm
0.1% Mn, cooled	6.6	5.3	1.55×10^{-8}
0.3% Mn, cooled	7.5	7.5	8.43×10^{-12}
0.6% Mn, cooled	8.1	6.5	7.08×10^{-11}
0.1% Mn, annealed	5.8	2.0	1.10×10^{-7}
0.3% Mn, annealed	6.6	3.1	9.33×10^{-9}
0.6% Mn, annealed	7.0	3.9	1.65×10^{-9}

4. Discussion

As discussed in a previous paper,[5] the amount of impurities present in ZnO, other than Mn, is not enough to interfere with the ZnO electrical properties in the case of quenched samples. In fact, the amount of Mn (2–3 orders of magnitude higher than the others) is so high that it controls the ZnO defect chemistry at the sintering temperature. The determination of its energy level (around 2.0 eV below the conduction band edge at room temperature), assuming that Mn is a donor in ZnO, nicely agrees with other types of experiments.[11–13] Furthermore, the calculation in the previous paper showed that Mn depresses the concentration of the intrinsic ZnO donors, assumed to be the zinc interstitials, at the sintering temperature. At room temperature, Mn-doped samples become more resistive because the concentration of the zinc interstitial was reduced. This is the case observed in Fig. 2b. When the samples are slowly cooled (Fig. 2a), they show a varistor behaviour, with high resistivity at low applied voltage and fairly important α values ($\geqslant 6$). Since no segregation of Mn was observed in these samples by TEM, the varistor behaviour can not be directly assigned to this dopant by itself, and must be related to the intrinsic defects of ZnO.

This first conclusion agrees with the assumption made by Einzinger[14] that varistor properties should be observed in undoped ZnO sintered in a very high oxygen partial pressure, providing an oxidation of the grain boundaries and keeping the bulk as a n-type semiconductor. These are difficult experimental conditions to attain, the reason why Einzinger's model was not later explored. The author[6] later proposed that the oxidation of the grain boundaries could be done by the presence of foreign donors in this region, hindering the concentration of intrinsic donors (assumed to be the oxygen

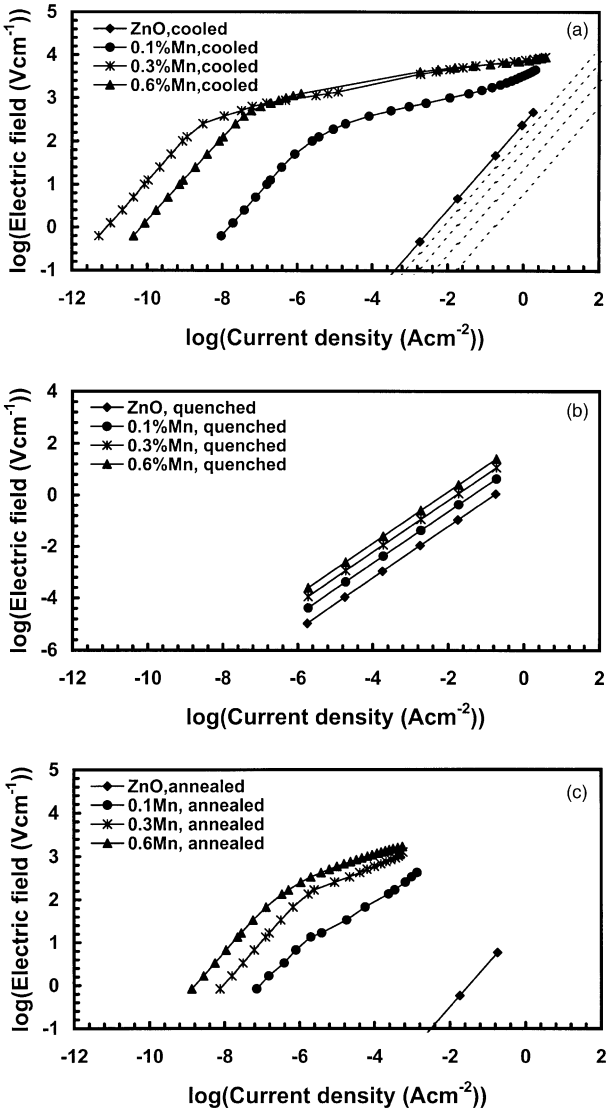

Fig. 2. Current density-electric field (dc J–E) characteristics of undoped and Mn-doped ZnO sintered at 1200 °C for 2 h, for (a) slowly cooled samples, (b) quenched samples, and (c) annealed samples. The dashed lines in a) represent the quenched samples for comparison.

vacancies) in such a way that its concentration could be less than that of the intrinsic acceptors (the zinc vacancies), thereby creating a potential barrier. In this last model, the intrinsic defects must migrate from the bulk to the grain boundaries in order to be annihilated during the cooling process. Mahan[15] showed later that this defect-migration mechanism could account for only $\leqslant 0.1$ eV for the barrier height in the material, a small contribution compared with the normally observed values (>0.7 eV). The same conclusion was drawn by Baptista et al.,[16] although it was demonstrated that this mechanism could account for the influence of the grain size on the final electrical characteristics of the material, provided that the zinc interstitial is the main intrinsic donor in ZnO. Using the experimental data of Philipp and Levinson,[17] Baptista and Mantas[18] showed that the Fermi energy level at the grain boundaries in equilibrium (without an applied voltage) is kept near the middle of the band gap down to around 700 °C, i.e. the grain boundary region behaves as an insulating stoichiometric material down to this temperature, probably due to an oxidation reaction with ambient oxygen. This process results in a barrier height of $\sim$0.8 eV at room temperature. The simplicity of the chemical composition used in this work, and the fact that the dopant (Mn) is not segregated at grain boundaries, should help us to better understand this process.

In Fig. 2a, the bulk resistivities of Mn-doped ZnO samples should be "observed" in the linear upturn region of the I–V curves. This upturn region is not explicitly seen in Fig. 2a, and it should be observed for even higher electric fields, which is not achieved in the present experimental conditions. However, from Fig. 2a, it is reasonable to estimate that the bulk resistivity of the doped samples is close to the resistivity of the undoped ZnO. When samples are slowly cooled from the sintering temperature, the equilibrium condition in the bulk can be maintained down to a temperature where it is still kinetically possible for the defect reactions to take place, below which only electrons and holes are in equilibrium, i.e. ionic defects become frozen at this temperature. In other words, during slow cooling, before arriving at the freezing temperature, the defect concentrations can keep the equilibrium values which decrease with decreasing the temperature. In Einzinger's[6] and Mahan's[15] models, the authors assumed that oxygen vacancies were the main intrinsic donors in ZnO. Therefore, the decrease in the concentrations of the oxygen vacancies in the bulk during slow cooling can only be performed by the migration of the oxygen vacancies from the bulk to the grain boundaries in order to be annihilated. However, as discussed in a previous work,[5] we assumed that the dominant intrinsic donors are the zinc interstitials coming from the Frenkel reaction of the Zn sublattice, rather than the oxygen vacancies. In this way, the zinc interstitials can be annihilated during slow cooling in the bulk of the material by the following reaction, without the migration of the zinc interstitials to the grain boundaries:

$$Zn_i + V_{Zn} \Longleftrightarrow Zn_{Zn} \tag{2}$$

In this reaction, where Kröger–Vink's notation is used, we explicitly omitted the charge of the defects. Although it can not be ruled out the contribution of the defect-migration mechanism to the bulk resistivity of the material, as a first approximation we shall assume that the defect freezing temperature determines the bulk resistivities of the samples at room temperature. Therefore, we can calculate the freezing temperatures for the bulk of Mn-doped samples. In a previous work,[5] we gave a detailed procedure for calculating the bulk electron concentrations of the samples at room temperature

from the defect freezing temperature, based on a proposed defect model. In that work, the concentrations of the bulk electrons and other defects were firstly calculated at the freezing temperature by solving the electroneutrality function with the defect reaction constants in the model. Then the bulk electron concentrations at room temperature were obtained by solving the electroneutrality function and using the freezing ionic defect concentrations. In the present work, as mentioned before, we estimate that for the slowly cooled case, the bulk resistivities of the doped samples are approximately equal to the resistivity of the undoped sample (Fig. 2a). Therefore, the bulk electron concentrations of the slowly cooled samples can be calculated from the resistivities, assuming 100 $cm^2\ V^{-1}\ s^{-1}$ for the electron mobility in the bulk at room temperature. Using the same method previously described,[5] for the slowly cooled samples, we calculated the bulk electron concentrations at room temperature from a given freezing temperature, and then compared these concentrations with those calculated from the bulk resistivities. If these two concentrations were not equal, we adjusted the freezing temperature and re-calculated the bulk electron concentrations until they became equal. By this way, the calculations determined the freezing temperatures of $\sim$1090, $\sim$1140 and $\sim$1170 °C, for the 0.1, 0.3 and 0.6 mol% MnO, respectively. Considering the error on the estimation of the bulk resistivities of the slowly cooled samples, these results show that the freezing temperatures are close to the sintering one, 1200 °C, which means that even reaction (2) hardly proceeds during cooling, not to mention the migration of defects. In fact, the J–E curves of the quenched samples (Fig. 2a, dashed lines) are in the same region where one should observe the upturn regions of the varistors. It means that the bulk resistivities of the slowly cooled samples are close to the resistivities of the quenched samples. Thus, it seems clear there is not any migration of defects to the grain boundaries during the cooling period, or, if present, this process could be neglected in the overall computations for the barrier height formation.

The above conclusions, together with the facts that there is no segregation of Mn in the grain boundaries and that Mn is not ionised at room temperature, do not enable one to assume that varistor properties in this simple chemical system arise from the ionisation of surface states formed by Mn. As previously reported,[18] one possibility for the growth of a barrier height comes from the oxidation of the grain boundaries by ambient oxygen. Since we are considering that the main intrinsic donor is the zinc interstitial, the oxidation can proceed by the following reaction,

$$Zn_i + \frac{1}{2}O_2(g) \Longleftrightarrow ZnO \qquad (3)$$

where again we explicitly omitted the defect charge. The decrease of the zinc interstitial concentration near the grain boundaries by reaction (3) will lead to a decrease of the electron concentration in this region, which results in a band bending and the appearance of a barrier height.

This very simple process for the formation of the barrier height must be confronted to the fact that undoped ZnO does not show varistor behaviour, and by reaction (3) this behaviour should be present even in this case. It is then clear that the presence of Mn enhances reaction (3) to proceed to the right side. However, varistor behaviour is also observed if ZnO is doped with Bi_2O_3 or other "varistor forming" elements, and due to the difference in chemical systems, it is more reasonable to expect that the process has an "intrinsic" origin. As explained before,[5] Mn changes the defect chemistry of ZnO, and therefore we should analyse this to found the possible intrinsic defect responsible for reaction (3) to proceed. Fig. 2c represents the room temperature J–E curves of the annealed samples, and it is observed that only the Mn-doped samples show a varistor behaviour. It is also observed that the leakage current decreases with increasing the Mn content in the annealed samples (Fig. 2c and Table 1), which means that the equilibrium Fermi level at the interface, E_{Fb0}, is lower in energy (relative to the valence band edge). E_{Fb0} is equal to E_{Fg0}-eΦ_{B0}, where E_{Fg0} is the equilibrium Fermi level in the bulk, and eΦ_{B0} the equilibrium barrier height. We stated above that the potential barrier, eΦ_{B0}, is not directly related to the presence of Mn. Therefore, the observed changes of E_{Fb0} in the annealed samples must be related to changes in E_{Fg0}, i.e. E_{Fg0} should be lower as the Mn content is higher. Fig. 3 depicts qualitatively this situation. The defect chemistry model[5] allows us to determine the equilibrium Fermi levels in the bulk at room temperature of the quenched samples, and we assume these to be equal to the bulk Fermi levels of the annealed samples, E_{Fg0}, since there is no change of the defect equilibrium in the bulk after annealing. Using the double Schottky barrier (DSB) model developed by Blatter and Greuter,[19] in the same way as reported before,[4] we can calculate the equilibrium Fermi level at the interface, E_{Fb0}, from the experimental I–V curves. In this calculation, the values of $(e\Phi_B + \varepsilon_\xi)$ were determined by successive fittings of the theoretically calculated I–V curves, i.e. $J_{dc} = A^*T^2\exp(-(e\Phi_B + \varepsilon_\xi)/kT)(1-\exp(-eV/kT))$, to the experimental ones, where ε_ξ is the Fermi energy in the bulk from the conduction band edge, J_{dc} the current density, A^* the Richardson constant, T the absolute temperature, e the electron charge, k the Boltzmann constant, and V the applied voltage. Then the values of E_{Fb0} were obtained due to $E_{Fb0} = E_g - (e\Phi_B + \varepsilon_\xi)$, where E_g is the band gap energy. Finally, the room temperature barrier heights of the annealed samples were determined, i.e. $e\Phi_{B0} = E_{Fg0} - E_{Fb0}$. The calculations gave $e\Phi_{B0} = \sim 0.50$ eV for all of the Mn-doped samples,

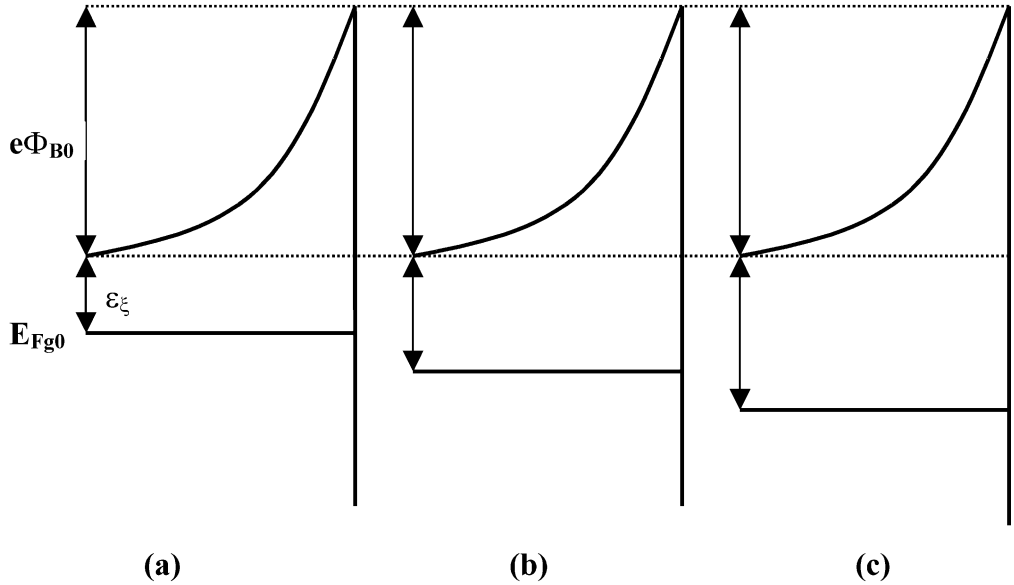

Fig. 3. Energy band diagram qualitatively describing the situation of the annealed samples doped with (a) 0.1 mol% MnO, (b) 0.3 mol% MnO, and (c) 0.6 mol% MnO. It is assumed that the barrier height, $e\Phi_{B0}$, does not depend on the content of Mn. The Fermi energy in the bulk from the conduction band edge, $\varepsilon_\xi = E_g - E_{Fg0}$, is exaggerated to better show the influence of Mn on this parameter, where E_g is the band gap energy.

which quantitatively agrees with the previous qualitatively description depicted in Fig. 3. The important point here is to remark that the same process upon annealing took place in all the samples, independently on the Mn content, i.e. this process controls the barrier height.

Our next step is to assign the interstitial zinc species involved in reaction (3). Fig. 4 shows that the variation of the concentrations of the different defect species in ZnO with the Mn content, at room temperature, of the quenched samples. It is observed that in pure ZnO the main donor is the monoionised zinc interstitial, $Zn_i^{\bullet}$, while upon the addition of MnO its concentration decreases below that of the double ionised species, $Zn_i^{\bullet\bullet}$. Therefore, it seems reasonable to expect that the last species, $Zn_i^{\bullet\bullet}$, is responsible for the reaction with ambient oxygen, and reaction (3) can then be rewritten as follows

$$Zn_i^{\bullet\bullet} + 2e' + \frac{1}{2}O_2(g) \iff ZnO \qquad (3a)$$

If this reaction is taking place, the amount of $Zn_i^{\bullet\bullet}$. is even decreasing through

$$Zn_i^{\bullet} \iff Zn_i^{\bullet\bullet} + e' \qquad (4)$$

i.e. the grain boundary region is being depleted of charges.

We arrived at the conclusion that the same chemical potential is present in the oxidation process, and that this potential is related to the $Zn_i^{\bullet\bullet}$ species. This means that reaction (3a) will take place only when the Fermi level at the interface is below the energy level of this defect. However, if the amount of shallow donors is high, there is no oxidation of the grain boundaries during cooling because the Fermi level increases above that energy level. This mechanism explains why pure ZnO does not show a varistor behaviour, even in a slowly cooling process. The same is true for heavily Al-doped ZnO,[20] or other extrinsic shallow donor in ZnO. When the above mentioned experimental conditions are found, reaction (3a) proceeds and the material turns a varistor because the grain boundaries are depleted of charges. Looking again at Fig. 4, it is observed that the concentration of $Zn_i^{\bullet\bullet}$ species that will be oxidised upon annealing is 10^{14}–10^{15} cm^{-3} which is 4–5 orders of magnitude lower than the added concentration of Mn ($\sim 10^{19}$ cm^{-3}), a feature commonly observed in the case of varistors produced by doping ZnO with Bi.[21] Again, it can thus be concluded that the dopant does not play a direct role in the formation of the barriers at the grain boundaries, as one could expect a priori, but instead promotes the conditions necessary to form the barriers by controlling the defect chemistry of ZnO.

5. Conclusions

Undoped and Mn-doped ZnO samples were prepared and sintered at 1200 °C, for 2 h, in air. A set of samples was slowly cooled from the sintering temperature, and another set was quenched from that temperature. The slowly cooled Mn-doped samples showed varistor behaviour, with fairly pronounced non-linearity, $\alpha > 6$, while the quenched and the undoped ones showed ohmic behaviour.

Using a defect chemistry model presented elsewhere[5] in which the main defects are the zinc interstitial species

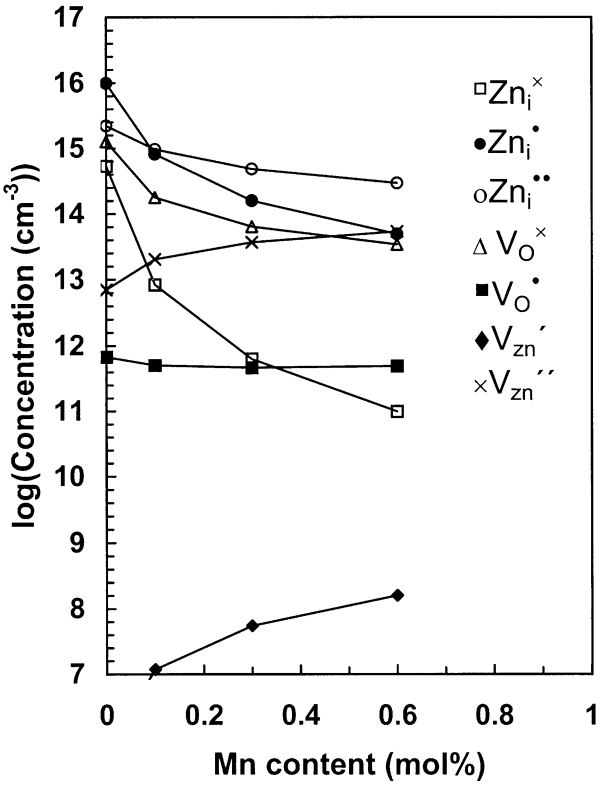

Fig. 4. Room temperature concentrations of the different intrinsic defects of ZnO as a function of the amount of Mn, for the samples quenched from 1200 °C. (Note: the concentrations of the defects V_O and $V_{Zn}^{\bullet\bullet}$ are too low to be shown in this figure.)

coming from a Frenkel reaction in the Zn sublattice, it could be concluded that the migration of defects to the grain boundaries during the cooling period is negligible. This, together with the experimental fact that Mn is homogeneously distributed in ZnO, pointed to the possibility that the varistor behaviour arose from an "intrinsic" mechanism.

The quenched samples were then annealed at 800 °C, for 2 h, in air, a process allowing the oxidation of the grain boundaries by ambient oxygen, without changes in the bulk defect chemistry conditions. Only Mn-doped samples showed varistor behaviour after this treatment, and it could be computed that the barrier height in those samples is not dependent on the Mn content. The result confirmed the assumption that varistor behaviour is not directly related to the presence of the dopant. The oxidation of the grain boundaries, proceeded by the elimination of the zinc interstitial species (the intrinsic donors in ZnO), and the analysis of the defect chemistry of undoped and Mn-doped ZnO allowed to conclude that the oxidation process takes place only when the majority of these species are double ionised. The amount of these species in varistor samples is several orders of magnitude lower than that of the MnO added, a similar situation observed in the case of Bi-doped ZnO varistor systems.[20]

As a final remark, one can say that in Mn-doped samples the varistor behaviour arises mainly by the oxidation of the double ionised zinc interstitials near the grain boundaries, and probably the same is true for any other dopants used to decrease the concentration of shallow donors below the deeper ones.

Acknowledgements

The author, J.H., would like to thank the financial support of the Praxis XXI programme of the Foundation for Science and Technology (FCT), Portugal.

References

1. Levinson, L. M. and Philipp, H. R., Zinc oxide varistors—A review. *Ceram. Bull.*, 1986, **65**, 639–646.
2. Gupta, T. K., Application of zinc oxide varistors. *J. Am. Ceram. Soc.*, 1990, **73**, 1817–1840.
3. Clarke, D. R., Varistor ceramics. *J. Am. Ceram. Soc.*, 1999, **82**, 485–502.
4. Mantas, P. Q. and Baptista, J. L., The barrier height formation in ZnO varistor. *J. Eur. Ceram. Soc.*, 1995, **15**, 605–615.
5. Han, J., Mantas, P. Q. and Senos, A. M. R., Defect chemistry and electrical characteristics of undoped and Mn-doped ZnO. *J. Eur. Ceram. Soc.,* in press.
6. Einzinger, R., Grain boundary phenomena in ZnO varistors. In *Grain Boundaries in Semiconductors, Mater. Res. Soc. Symp. Proc.*, ed. H. J. Leamy, G. E. Pike and C. H. Seager. Elsevier, New York, 1982, pp. 343–355.
7. Dallavalle, J. M., Particle- and grain-size distributions. In *Quantitative Stereology*, ed. E. E. Underwood. Addison-Wesley publishing company, Reading, Massachusetts, 1971, pp. 109–147.
8. Han, J., Senos, A. M. R. and Mantas, P. Q., Nonisothermal sintering of Mn-doped ZnO. *J. Eur. Ceram. Soc.*, 1999, **19**, 1003–1006.
9. Han, J., Mantas, P. Q. and Senos, A. M. R., Grain growth in Mn-doped ZnO. *J. Eur. Ceram. Soc.*, 2000, **20**, 2753–2758.
10. Morris, W. G. and Cahn, J. W., Adsorption and microphases at grain boundaries in non-ohmic zinc oxide ceramics containing bismuth oxide. In *Grain Boundaries in Engineering Materials*, ed. J. L. Walter, J. H. Westbrook and D. A. Woodford. Claitors, Baton Rouge, LA, 1975, pp. 223–234.
11. Kleinlein, F. W. and Helbig, R., Diffusion constant and typical near-band edge absorption of manganese in zinc oxide crystals. *Z. Phys.*, 1974, **266**, 201–207.
12. Jakani, M., Campet, G., Claviere, J., Fichou, D., Pouliquen, J. and Kossanyi, J., Photoelectrochemical properties of zinc oxide doped with 3d elements. *J. Solid State Chem.*, 1985, **56**, 269–277.
13. Fichou, D., Pouliquen, J., Kossanyi, J., Jakani, M., Campet, G. and Claviere, J., Extension of the photoresponse of semiconducting zinc oxide electrodes by 3d-impurities absorbing in the visible region of the solar spectrum. *J. Electroanal. Chem.*, 1985, **188**, 167–187.
14. Einzinger, R., Metal oxide varistor action—A homojunction breakdown mechanism. *Appl. Surf. Sci.*, 1979, **1**, 329–340.
15. Mahan, G. D., Intrinsic defects in ZnO varistors. *J. Appl. Phys.*, 1983, **54**, 3825–3832.
16. Baptista, J. L., Mantas, P. Q. and Frade, J. R., Grain boundary induced perturbation in electrical ceramics. In *Ceramic Transactions,* Vol. 71, ed. K. Kuomoto, L. M. Sheppard and H. Matsubara. American Ceramic Society, OH, 1996, pp. 61–77.
17. Philipp, H. R. and Levinson, L. M., High-temperature behavior

of ZnO-based ceramic varistors. *J. Appl. Phys.*, 1979, **50**, 383–389.
18. Baptista, J. L. and Mantas, P. Q., High temperature characterisation of electrical barriers in ZnO varistors. *J. Electroceram.*, 2000, **4**, 215–224.
19. Blatter, G. and Greuter, F., Carrier transport through grain boundaries in semiconductors. *Phys. Rev. B*, 1986, **33**, 3952–3965.
20. Han, J., Mantas, P. Q. and Senos, A. M. R., unpublished data.
21. Greuter, F. and Blatter, G., Electrical properties of grain boundaries in polycrystalline compound semiconductors. *Semicond. Sci. Technol.*, 1990, **5**, 111–137.